Published in final edited form as:
*J Surg Res*. 2013 January ; 179(1): e83–e90. doi:10.1016/j.jss.2012.02.037.

# Glucose Metabolism during the Early "Flow Phase" After Burn Injury

**Hongzhi Xu, MD, PhD**, **Yong-Ming Yu, MD, PhD**, **Harry Ma, MD, PhD**, **Edward A Carter, PhD**, **Shawn Fagan, MD**, **Ronald G. Tompkins, MD, ScD**, and **Alan J. Fischman, MD, PhD**
Department of Surgery, Massachusetts General Hospital, Harvard Medical School and Shriners Hospitals for Children, Boston MA

## Abstract

**Background—**Burn injury (BI) is associated with insulin resistance and hyperglycemia which complicate clinical management. We investigated the impact of BI on glucose metabolism in a rabbit model of burn injury using a combination of PET and stable isotope studies under Euglycemic Insulin Clamp (EIC) conditions.

**Materials/Methods—**Twelve male rabbits were subjected to either full thickness burn injury (B) or sham burn (SB). Three days after treatment, an EIC condition was established by constant infusion of insulin, concomitantly with a variable rate of dextrose infusion. PET imaging of the hind limbs was conducted to determine the rates of peripheral $O_2$ and glucose utilization. Each animal also received a primed constant infusion of [6,6,$^2H_2$] glucose to determine endogenous glucose production.

**Results—**The fasting blood glucose in the burned rabbits was higher than in the sham group. Under EIC conditions, the SB group required more exogenous dextrose than the B group in order to maintain blood glucose at physiological levels (22.2 ± 2.6 vs 13.3 ± 2.9 mg/min, $P < 0.05$), indicating a state of insulin resistance. PET imaging demonstrated that the rates of $O_2$ consumption and FDG utilization by skeletal muscle remained at similar levels in both groups. Hepatic gluconeogenesis determined by the stable isotope tracer study was found significantly increased in the BI group.

**Conclusions—**These findings demonstrated that hyperglycemia and insulin resistance develop during the early "flow phase" after BI. Unsuppressed hepatic gluconeogenesis, but not peripheral skeletal muscular utilization of glucose contributes to hyperglycemia at this stage.

### Keywords

PET; euglycemic insulin clamp; insulin resistance; stable isotopic tracer study

Address Correspondence to: Hongzhi Xu, MD, PhD Research Department Shriners Hospitals for Children Boston MA 02114 Phone: (617) 2793273 FAX: (617) 3714927 hongzhi2008@gmail.com.

## INTRODUCTION

Each year approximately 500,000 patients with burn injuries receive medical treatment in the U.S(1). Modern advances in the initial emergency and subsequent supportive care have significantly reduced mortality in this patient population. However, post-burn complications such as poor wound healing (2), skin graft loss (3), increased incidence of infections (4, 5) and muscle wasting (6) remain as major challenges for clinicians. Various studies have demonstrated that insulin resistance (IR) induced hyperglycemia plays a key role in the development of these adverse outcomes in post-burn patients (7) In order to fine-tune current clinical therapies or to design innovative treatment strategies, a clear understanding of alterations in glucose metabolism associated with IR is absolutely required. However, detailed information, such as the impact of IR on regional glucose disposal and how this contributes to systemic hyperglycemia are yet to be elucidated.

The Euglycemic Insulin Clamp (EIC) technique is a well-accepted method for quantitative assessment of tissue sensitivity to insulin. Under the hyper-insulinemic conditions, insulin levels are raised and the plasma glucose concentration is held constant at basal levels by a variable glucose infusion using the negative feedback principle. Under these steady-state conditions of euglycemia, the glucose infusion rate equals the rate of glucose uptake by all tissues of the body and is therefore a measure of tissue sensitivity to exogenous insulin. Additional information about whole body glucose metabolism, such as the rate of endogenous glucose production, can be obtained by simultaneous infusion studies with stable isotope labeled glucose. However, neither technique by itself allows for direct monitoring of glucose metabolism in individual tissues. In contrast, Positron Emission Tomography (PET) is a quantitative imaging technique that allows the acquisition of physiological images based on the detection of radiation from the emission of positrons. With radio-labeled glucose analogs such as $^{18}$F 2-fluoro-2-deoxy–D-glucose (FDG), it is possible to directly evaluate the metabolic fate of glucose in individual tissues, such as skeletal muscle *in vivo*. Thus, the combination of stable isotope studies and PET under EIC can provide a multi-dimensional picture of glucose metabolism *in vivo* in the same subject. Using these techniques, we investigated the impact of burn injury on glucose metabolism at two primary sites, liver and skeletal muscle in a rabbit model.

## MATERIALS AND METHODS

### Animals

12 male New Zealand white rabbits weighting 2.5-4.6 kg (Millbrook Farms, NY), were randomly assigned to sham burn ($n$ = 6) and burn ($n$ = 6) groups. On arrival, the animals were habituated to the environment for at least 48 h before use. All animals were kept in the Animal Farm of the Massachusetts General Hospital, under the care of the veterinary staff. Water and food (Prolab Hi-fiber Rabbit Chow, 5P25, PMI Nutritional International, Brentwood, MO) were provided *ad libitum*. The study protocol was approved by the Subcommittee on Research Animal Care and Use of the Massachusetts General Hospital.

### Burn Injury Model in Rabbits

Thermal injury was produced on the dorsal surface of the rabbits as described elsewhere (8). Briefly, the rabbits were anesthetized with ketamine (100 mg/kg) and xylazine (10 mg/kg) injected subcutaneously in the shoulder region. The dorsal surface was shaved and each animal was placed in a mold exposing 25% of the skin to water heated at 100°C for 15 sec. A full-thickness third degree burn wound was thus formed and was verified by histological examination. After injury, the animals were allowed to recover from anesthesia under fluid resuscitation (0.9% Sodium Chloride, i.v., 3ml / % TBSA for 4hrs). Sufficient analgesia was administered to minimize chronic pain-induced stress and associated metabolic alterations. These included: burprenorphine (0.02 mg/kg, i.m.) before burn injury administered together with anesthesia and every 12 hours thereafter, once cornea reflexes were recovered. In addition, ELMA™ cream (containing lidocaine and prilocaine, topical anesthesics for pediatric patients) was applied to the wound twice a day. A sham burn group which served as a control was treated in the same way as the burned animals; however, the exposed area was immersed in room temperature water for 15 seconds. After recovering from anesthesia the animals returned to their cages in the animal facility. Water and food are provided *ad libitum*

All metabolic studies were performed after fasting overnight on the third post-burn day. At this time, the rabbits had recovered from the acute phase of injury. They were free of sepsis, as evidenced by dry wounds and negative blood cultures.

### Experimental Design

The overall experimental design is summarized in Figure 1 and described in detail below.

### Surgical Preparation

After overnight fasting, the rabbits were anesthetized with ketamine (10mg/kg, i.m.) and xylazine (4mg/kg, i.m.) and anesthesia was maintained by constant inhalation of 2% Isoflurane via an anesthesia machine (Model: VMS Matrix, Midmark Corp, Versailles, OH). Polyethelene catheters (ID 0.034”, Clay Adames Parsipany, NJ) with 3 cm silastic tips (ID 0.30 in. Don Corning, Midland Me) were implanted into the left jugular vein and carotid artery through a 1.5 cm vertical incision in the neck region, using aseptic procedures. A tracheotomy was performed, and an infant endo-tracheal tube (10 cm long) was inserted 3 cm into the trachea and secured with a silk ligature. Heart rate, mean arterial blood pressure, and rectal temperature were maintained at stable levels by adjusting the anesthesia and a heating pad. These vital signs were recorded every 30 min. Blood gasses were monitored with a vet Oximeter (SDI VET/OX Plus 4500/4600, SDI Sensor Devices Inc. Waukersha, WI) throughout the study. Euthanasia were performed by intravenous injection of an overdose of pentobarbital (>150mg/kg).

### Stable Isotope Tracer Study

After surgical preparation, a blood sample was collected for the measurements of baseline stable isotope enrichments at the beginning of the study. Each animal then received a primed constant tracer infusion of [6,6,$^{2}H_{2}$] glucose with a priming dose of 80 μmol/kg and a

targeted infusion rate of 1 μmol/kg/min, for 4 hrs. Arterial blood samples, 2 ml each, were collected at 100, 110, 120, 220, 230, 240 min after starting the tracer infusion. At the conclusion of the study the animals were euthanized and total weight of the hind-limbs, skin, bone and muscle were measured and their proportions to whole body weight were calculated.

### Euglycemic Insulin Clamp

The clamp was started at 120 min after initiation of stable isotope tracer infusion. The procedure was similar to that described by Zhang et al (9) with slight modifications. Briefly, a bolus injection of 50 mU/kg insulin (Humulin R Eil Lilly, Indianapolis, IN) was injected into the external jugular vein and was followed immediately by an infusion of insulin in 0.25% human serum albumin at a rate of 4.5 mU/kg/min. Approximately 4-5 minutes after insulin administration, an infusion of 25% dextrose was begun with an initial pump setting of 0.1 ml/min which was adjusted every five minutes based on plasma glucose levels. Plasma glucose levels were monitored with a glucose analyzer (Bayer HealthCare LLC, Mishawaka, IN) and were maintained at 90-120 mg/dl (5-6.7 mM).

### PET Imaging and Data Analysis

Once the steady state of euglycemia was achieved ~30 minutes after initiation of the EIC, the rabbits were positioned in the gantry of a PC-4096 PET camera (Scanditronix AB, Sweden) with their thighs centered in the field of view. The imaging characteristics of this instrument and the parameters for image reconstruction (10-12) have been well-described in the literature. Radioactive gases were supplied to a cylindrical mixing chamber (2.5 cm diameter × 4.5 cm), which was placed over the nose, mouth and endotracheal tube. All rabbits were studied consecutively with inhalation of $C^{15}O_2$, which produces radiolabeled water *in vivo* (via carbonic anhydrase), for measuring blood flow; $^{15}O_2$ for measuring oxygen utilization; and intravenous injection of $^{18}$FDG for measuring glucose metabolism. The concentration of radioactivity in arterial blood was monitored continuously with a pair of coincidence detectors placed in a loop between the arterial and venous catheters. Regions of interest (ROIs) of the same size and shape were drawn over the thigh muscle and average values for blood flow and oxygen utilization were calculated using previously described methods (13, 14).

The same ROIs that were used for calculating blood flow and oxygen utilization were used for calculating glucose metabolic rate, which was evaluated by a 3-compartment, 3 rate constant model of FDG kinetics as described previously (15) with a value of 0.5 for the lumped constant (16). Briefly, when $^{18}$FDG is injected, it is transported from plasma into cells according to the rate constant $K_1$, transported back into plasma with the rate constant $k_2$, phosphorylated with a rate constant $k_3$ and dephosphorylated with a rate constant $k_4$. Since, $^{18}$FDG-$PO_4$ cannot proceed further in glycolysis or be used for glycogen synthesis, tracer accumulation reflects glucose utilization. From measurements of the time dependence of tissue (PET) and plasma radioactivity, the differential equations described by the model can be solved to yield values for $K_1$ and $k_{2\text{-}4}$. For tissues with minimal glucose-6-phosphatase activity (brain, heart, muscle etc), the rate of glucose metabolism ($MR_{Glc}$, μmole/min/g) can be calculated using the relation:

$$\mathbf{MR_{Glc}}=\frac{\mathbf{C_p}}{\mathbf{LC}}\left[\frac{\mathbf{k_1 k_3}}{\mathbf{K_2}+\mathbf{k_3}}\right] \quad (1)$$

Where $C_p$ is the plasma glucose concentration and *LC* is the "lumped constant" that corrects for the differences in kinetic behavior between $^{18}$FDG and glucose.

## Sample Treatment and Mass Spectroscopic Analysis

The blood samples from each experiment were immediately centrifuged and the supernatants were preserved at −80°C until analysis. The procedure for preparation of di-*O*-sopropylidene derivatives were similar to those previously described by Hachey DL et al (17). Briefly, plasma was mixed with cold acetone (0 °C), followed by centrifugation at 2000 × g for 5 min to remove plasma proteins. The di-*O*-isopropylidene ester was formed by acetonation with 0.38 M sulfuric acid followed by extraction with ethyl acetate and acylation with acetic anhydride (1:1) at 60 °C for 60 min. The blood enrichments of [6, 6-$^2H_2$] glucose were determined by gas chromatography mass spectrometry (GC-MS, Hewlett-Packard, 5985B) using electron ionization (EI) mode. The concentration of blood glucose was determined using mass abundance ratio of natural glucose versus internal standard D-Glucose-2,3,4,6,6 [(m+5 Glucose) (Merck Sharp& Dohme Canada Ltd.)] following previously described procedures (3).

## Calculation of Endogenous Glucose Production ($Endo_{glc}$)

Whole body glucose turnover rate ($Q_{glc}$) was determined with the steady-state isotope tracer dilution approach (18):

$$\mathrm{Q}_{glc}=\mathrm{i}_{glc}\left(\mathbf{E}_\mathrm{i}/\mathbf{E}_\mathrm{p}-1\right) \quad (2)$$

Where: $i_{glc}$ is the infusion rate of [6, 6-$^2H_2$] glucose, $E_i$ is the isotopic enrichment of [6, 6-$^2H_2$] glucose in the infusate and $E_p$ is the plateau level [6, 6-$^2H_2$] glucose enrichment.

At steady state:

$$\mathrm{Q}_{glc}=Exo_{glc}+Endo_{glc}, \quad (3)$$

Where $ExO_{glc}$ is the rate of glucose intake and $Endo_{glc}$ is the rate of endogenous glucose production. In the fasting basal state, $Exo_{glc}$ = 0, so $Endo_{glc}$ = $Q_{glc}$. During the euglycemic insulin clamp state, $Exo_{glc}$= $I_{dex}$, where $I_{dex}$ = infusion rate of dextrose.

Thus, endogenous glucose production ($Endo_{glc}$) can be calculated as:

$$Endo_{glc}=\mathrm{Q}_{glc}-\mathrm{I}_{dex} \quad (4)$$

## Statistical Analysis

All data were expressed as means ± SEM. Student's t tests were used to evaluate differences between the burn and sham burn groups. A P value < 0.05 was considered to be statistically

significant. The effect of burn injury and EIC on the rate of endogenous glucose production was evaluated by two-way ANOVA.

## RESULTS

All animals survived the burn injury. The average body weight of the rabbits on the third postburn day was not significantly different from that before burn. The wound surface was dry (unlike in human burn, there were no blisters, or surface exudates) with sharp edges and the burned surface showed gray color. The arterial blood pressure remained constant (90-110/60-70 mmHg) throughout the experimental period.

### Blood Glucose Levels Before and After EIC

Three days after burn injury, the average basal blood glucose level (i.e. levels during phase I) was 223.5 ± 25.4 mg/dl which was significantly elevated comparing with the sham burn group in which the glucose level was 147.5 ± 21.5 mg/dl ($P < 0.05$, see Figure 2). This indicates that hyperglycemia exists at 3 days after burn injury. During the Euglycemic Insulin Clamp stage (phase II), average blood glucose levels of both groups were maintained at similar levels (111.7 ± 6.3 vs. 106.9 ± 6.5 mg/dl, see Figure 2).

At the beginning of the Euglycemic Insulin Clamp, infusion of 25% dextrose solution was initiated shortly after insulin administration. The infusion rate for the burn group was markedly lower than that for sham group in order to keep blood glucose at euglycemic levels (4.1 ± 0.9 vs. 6.9 ± 0.6 mg/min/kg, $P < 0.05$, see Figure 3), indicating a blunted response to the hyperinsulinemic condition from either liver or peripheral tissue or both (i.e. an insulin resistance) in three-day post-burn animals.

### PET Study of Glucose Uptake, Oxygen Extraction Fraction and Blood Flow in Hind Limb Skeletal Muscle

The rate of glucose utilization, oxygen extraction fraction (OEF) and blood flow in hind-limb skeletal muscle during the EIC are summarized in Figure 4. We found except that blood flow to hind limb muscle was significantly increased in burned rabbits (3.8 ± 0.4 vs. 2.2 ± 0.4 ml/min/kg, $P < 0.05$ Figure 4C), muscular glucose utilization rate and OEF was similar in both sham burn and burn groups (Glucose Utilization rate: 39.3 ± 4.8 vs. 45.5 ± 7.9 μmol/min/kg, $P > 0.05$ Figure 4A; and OEF: 84.6 ± 17.7% vs. 86 ± 13.3%, $P > 0.05$ Figure 4B). Because the efficacy of glucose utilization (e.g. uptake and oxidation) in local muscular tissue reflects the extent of insulin resistance in this region, the relatively unaffected muscular tissue glucose utilization after burn injury implies that the major manifestation of insulin resistance, as suggested by the EIC study, may be elsewhere other than the peripheral muscle tissue.

### Changes in Endogenous Glucose Production after EIC

Using stable isotope tracer technique, we found that the levels of endogenous glucose production were significantly elevated in burn injured rabbits compared with the sham treated group (13.6 ± 1.7 vs. 9.1 ± 1.0 mg/kg/min; $P < 0.05$) (Figure 5). Under fasting conditions, the main source of endogenous glucose production is the gluconeogenesis from

the liver. Thus, this elevated endogenous glucose production under insulin clamp condition suggests the effect of insulin in suppressing hepatic gluconeogenesis is compromised after burn injury, which may at least partially contribute to the overall insulin resistance state.

## DISCUSSION

Hyperglycemia has been documented as one of the major characteristics of burn injury (19). Rather than being beneficial as previously believed, burn-induced hyperglycemia may be a significant risk factor since it has been linked to various adverse clinical complications (20). Therefore, it is important to have a better understanding of the factors associated with the development of post-burn hyperglycemia. Essentially, hyperglycemia is a result of imbalance between glucose production and glucose utilization in the body. In the present study, using PET imaging in combination with stable isotopic tracer and euglycemic insulin clamp techniques, we obtained detailed evidence that hyperglycemia after burn injury is mainly due to increased endogenous glucose production, rather than reduced glucose utilization or disposal by skeletal muscle during the early flow phase of burn injury.

Previous studies have suggested that there are two distinct phases of metabolic alterations following burn injury: the “ebb phase” which occurs within the first 48 hours after injury followed by the “flow phase” that is characteristically associated with a hypermetabolic state. In general, profound metabolic alterations responsible for many clinical complications primarily occur during the “flow phase”. Previously we developed a rabbit burn model, in which a significant elevation of resting energy expenditure and accelerated proteolysis was observed on the third post-burn day; mimicking the metabolic pattern of the early “flow phase” in burn patients (21). Thus we used this three-day post burn model to further study the impact of burn injury on glucose metabolism. Consistent with the results of the previous studies, the fasting glucose concentration was increased in the burned animals. Moreover, using the euglycemic insulin clamp technique, we demonstrated that tissue responsiveness to insulin was markedly attenuated, indicating that a state of insulin-resistance had already developed at three days after burn injury.

A wealth of clinical and experimental data has suggested that insulin resistance plays a pivotal role in the pathophysiology of aberrant glucose metabolism after burn injury. Pro-inflammatory cytokines (22), stress hormones (23) and oxidative stress (24) have been shown to contribute to the development of insulin resistance, by directly or indirectly impairing the insulin signaling pathway or GLUT-4 translocation. The impact of insulin resistance on glucose metabolism is manifested in two ways; unsuppressed hepatic gluconeogenesis and impaired peripheral glucose utilization. Previous work by Kidrasova et al (25) and Wilmore et al (26) revealed that hepatic gluconeogenesis is increased in rats and humans with burn injury. In line with their findings, the present study using the euglycemia insulin clamp technique demonstrated that: 1) the amount of exogenous glucose required to maintain euglycemia was less in burned animals compared to sham burn animals, indicating an insulin resistance state; however, 2) with the help of stable isotope tracers, the present study demonstrated that endogenous glucose production was much higher in animals with burn injury. Obviously, the increased hepatic glucose production is one of the manifestations of the insulin resistance state after thermal injury.

With regard to the peripheral utilization of glucose, the present study using PET techniques demonstrated that utilization of glucose by muscle tissues was not significantly altered after burn injury; this finding was consistent with the observation using stable isotope tracers that glucose clearance rate was not compromised after burn injury. Previous studies have reported that glucose disposal in peripheral tissues such as skeletal muscles might be altered after burn injury (27, 28). Thomas et al. observed a significantly decreased glucose uptake rate in rat skeletal muscle 5 days post-burn (29). We (12) and others (30) have also reported impaired peripheral glucose uptake at 3 wks or even months after burn injury. In contrast, in the early stage of the flow phase, there is no significant change in glucose uptake by skeletal muscle, as we demonstrated in the present study. Furthermore, Turinsky et al found that the uptake of glucose by muscle was not significantly changed despite the existence of insulin resistance using a 2-4 day post-burn rat model (31). Taken together, our data demonstrated that at three days post-burn, there was elevated hepatic gluconeogenesis while glucose uptake by skeletal muscles was not significantly altered. Post burn insulin resistance is a dynamic process with differential manifestations at different stages after injury: unsuppressed hepatic gluconeogenesis may precede decreased uptake of glucose by skeletal muscle at the early stage of the flow phase after burn injury. Currently, the underlying mechanism(s) for these sequential events are unclear. We speculate that direct effects of stress hormones (e.g. glucagon) that are usually elevated shortly after burn injury on gluconeogenesis (32) and/or heterogeneity of insulin sensitivity in different tissues (33, 34) might contribute to early unsuppressed hepatic glucose production.

The present study applied combined PET and stable isotope tracer methods to study glucose metabolism in burn and sham burn animals under fasting conditions and euglycemic insulin clamp status. This approach provided a number of advantages. Firstly, previous studies of muscle substrate metabolism have used measurements of A-V differences in tracer concentrations across the limbs (35) which are quite invasive. Secondly, in all A-V difference studies, accurate measurement of blood flow rate across the limb has been difficult. Thirdly, catheterization of the vessels may produce changes in blood flow. Fourthly, the measurements are not specific for muscle with contributions from skin and bone. In contrast, the PET approach is less invasive without the need for inserting catheters, Moreover PET allowed us to “visualize” glucose kinetics which specifically occur in skeletal muscle, not including bone and skin (10,11). Previous studies have utilized the combination of PET with insulin clamp to elucidate changes in regional glucose utilization in skeletal muscle in insulin resistant states such as obesity (36), non-insulin-dependent diabetes mellitus (37) and liver cirrhosis (38). In the present study, the combination of PET with stable isotope tracers allowed us to simultaneously evaluate the rate of endogenous glucose production and peripheral utilization in vivo. When these studies were conducted under both fasting and euglycemic clamp conditions, critical information about insulin resistance under the burn and sham burn conditions was obtained.

In the present study, PET imaging using $C^{15}O_2$ demonstrated a significant increase in blood flow in skeletal muscle under hyperinsulinemic conditions (36, 39). Previously, several studies have documented a similar effect in skeletal muscle in response to insulin in both animal models and humans (35, 40, 41). Liang et al suggested that this enhancement in local blood flow might be attributed to the direct vasodilator effect of insulin on skeletal muscle

vasculature (40). On the other hand, thermal injury itself has been reported to be associated with an increase in skeletal muscle arteriolar blood flow distant from the site of injury in rats (42). Clearly, additional studies are required to elucidate the underlying mechanism(s) responsible for increased blood flow in skeletal muscle after burn injury.

In summary, the present study demonstrated a significantly increased endogenous glucose production, without significant changes in muscle glucose utilization in thermally injured animals. The findings indicate that burn induced hyperglycemia and insulin resistance state predominantly occur in the liver. The combined PET-stable isotope approach allowed us to simultaneously evaluate glucose metabolism in vivo in liver and muscle. Because of the accuracy and less invasive nature, this technique is potentially applicable to future studies in health human volunteers and burn patients.

## Acknowledgments

The authors express their thanks to the technical assistance of Mr. James S. Titus and Ms. Florence Min Lin in preparing the animal model and mass spectrometry analysis.

## Abbreviations

| | |
|---|---|
| **PET** | Positron Emission Tomography |
| **FDG** | $^{18}$F 2-fluoro-2-deoxy–D-glucose |
| **EIC** | euglycemic insulin clamp |
| **IR** | insulin resistance |

## REFERENCES

1. American Burn Association/American College of Surgeons. Guidelines for the operation of burn centers. J Burn Care Res. 2007; 28:134–141. [PubMed: 17211214]
2. McMurry JF Jr. Wound healing with diabetes mellitus. Better glucose control for better wound healing in diabetes. Surg Clin North Am. 1984; 64:769–778. [PubMed: 6433493]
3. Mowlavi A, Andrews K, Milner S, Herndon DN, Heggers JP. The effects of hyperglycemia on skin graft survival in the burn patient. Ann Plast Surg. 2000; 45:629–632. [PubMed: 11128762]
4. Gore DC, Chinkes D, Heggers J, Herndon DN, Wolf SE, Desai M. Association of hyperglycemia with increased mortality after severe burn injury. J Trauma. 2001; 51:540–544. [PubMed: 11535907]
5. Tuggle DW, Kuhn MA, Jones SK, Garza JJ, Skinner S. Hyperglycemia and infections in pediatric trauma patients. Am Surg. 2008; 74:195–198. [PubMed: 18376680]
6. Gore DC, Chinkes DL, Hart DW, Wolf SE, Herndon DN, Sanford AP. Hyperglycemia exacerbates muscle protein catabolism in burn-injured patients. Crit Care Med. 2002; 30:2438–2442. [PubMed: 12441751]
7. Gauglitz GG, Herndon DN, Kulp GA, Meyer WJ 3rd, Jeschke MG. Abnormal insulin sensitivity persists up to three years in pediatric patients post-burn. J Clin Endocrinol Metab. 2009; 94(5): 1656–64. [PubMed: 19240154]
8. Vega GL, Baxter CR. Induction of hypertriglyceridemia in rabbits by thermal injury: I. Time course of elevated plasma triglyceride levels. J Burn Care Rehabil. 1988; 9:266–270. [PubMed: 3138242]
9. Zhang XJ, Chinkes DL, Doyle D Jr. Wolfe RR. Metabolism of skin and muscle protein is regulated differently in response to nutrition. Am J Physiol. 1998; 274:E484–492. [PubMed: 9530132]

10. Fischman AJ, Hsu H, Carter EA, Yu YM, Tompkins RG, Guerrero JL, Young VR, Alpert NM. Regional measurement of canine skeletal muscle blood flow by positron emission tomography with $H_2{}^{15}O$. J Appl Physiol. 2002; 92:1709–1716. [PubMed: 11896041]
11. Fischman AJ, Yu YM, Livni E, Babich JW, Young VR, Alpert NM, Tompkins RG. Muscle protein synthesis by positron-emission tomography with L-[methyl-$^{11}$C]methionine in adult humans. Proc Natl Acad Sci U S A. 1998; 95:12793–12798. [PubMed: 9788993]
12. Carter EA, Tompkins RG, Hsu H, Christian B, Alpert NM, Weise S, Fischman AJ. Metabolic alterations in muscle of thermally injured rabbits, measured by positron emission tomography. Life Sci. 1997; 61:39–44. [PubMed: 9200667]
13. Frackowiak RS, Lenzi GL, Jones T, Heather JD. Quantitative measurement of regional cerebral blood flow and oxygen metabolism in man using $^{15}$O and positron emission tomography: theory, procedure, and normal values. J Comput Assist Tomogr. 1980; 4:727–736. [PubMed: 6971299]
14. Lammertsma AA, Jones T. Correction for the presence of intravascular oxygen-15 in the steady-state technique for measuring regional oxygen extraction ratio in the brain: 1. Description of the method. J Cereb Blood Flow Metab. 1983; 3:416–424. [PubMed: 6630313]
15. Nelson KM, Turinsky J. Effect of insulin on glucose and amino acid uptake by skeletal muscle following burn injury. Studies with 2-deoxyglucose and alpha-aminoisobutyric acid. JPEN J Parenter Enteral Nutr. 1982; 6:3–8. [PubMed: 7043015]
16. Zhang XJ, Chinkes DL, Doyle D Jr, Wolfe RR. Metabolism of skin and muscle protein is regulated differently in response to nutrition. Am J Physiol. Mar; 1998 274(3 Pt 1):E484–92. [PubMed: 9530132]
17. Hachey DL, Parsons WR, McKay S, Haymond MW. Quantitation of monosaccharide isotopic enrichment in physiologic fluids by electron ionization or negative chemical ionization GC/MS using di-O-isopropylidene derivatives. Anal Chem. 1999; 71:4734–4739. [PubMed: 10546538]
18. Brainard JR, Downey RS, Bier DM, London RE. Use of multiple 13C-labeling strategies and 13C NMR to detect low levels of exogenous metabolites in the presence of large endogenous pools: measurement of glucose turnover in a human subject. Anal Biochem. 1989; 176:307–312. [PubMed: 2742122]
19. Oakes DD, Schreibman PH, Hoffman RS, Arky RA. Hyperglycemic, nonketotic coma in the patient with burns: factors in pathogenesis. Metabolism. 1969; 18:103–109. [PubMed: 5766385]
20. Mecott GA, Al-Mousawi AM, Gauglitz GG, Herndon DN, Jeschke MG. The role of hyperglycemia in burned patients: evidence-based studies. Shock. 33:5–13. [PubMed: 19503020]
21. Wilmore DW. Carbohydrate metabolism in trauma. Clin Endocrinol Metab. 1976; 5:731–745. [PubMed: 797486]
22. del Aguila LF, Claffey KP, Kirwan JP. TNF-alpha impairs insulin signaling and insulin stimulation of glucose uptake in C2C12 muscle cells. Am J Physiol. 1999; 276:E849–855. [PubMed: 10329978]
23. Hunt DG, Ivy JL. Epinephrine inhibits insulin-stimulated muscle glucose transport. J Appl Physiol. 2002; 93:1638–1643. [PubMed: 12381748]
24. Bitar MS, Al-Saleh E, Al-Mulla F. Oxidative stress--mediated alterations in glucose dynamics in a genetic animal model of type II diabetes. Life Sci. 2005; 77:2552–2573. [PubMed: 15936776]
25. Kidrasova RS, Kamilov F. [Effect of thermal injury on the gluconeogenesis in the liver and in the kidneys of immature animals]. Vopr Med Khim. 1982; 28:105–109. [PubMed: 7157711]
26. Wilmore DW, Mason AD Jr. Pruitt BA Jr. Insulin response to glucose in hypermetabolic burn patients. Ann Surg. 1976; 183:314–320. [PubMed: 1259488]
27. Burke JF, Wolfe RR, Mullany CJ, Mathews DE, Bier DM. Glucose requirements following burn injury. Parameters of optimal glucose infusion and possible hepatic and respiratory abnormalities following excessive glucose intake. Ann Surg. 1979; 190:274–285. [PubMed: 485602]
28. Wolfe RR, Durkot MJ, Allsop JR, Burke JF. Glucose metabolism in severely burned patients. Metabolism. 1979; 28:1031–1039. [PubMed: 491960]
29. Thomas R, Aikawa N, Burke JF. Insulin resistance in peripheral tissues after a burn injury. Surgery. 1979; 86:742–747. [PubMed: 494065]

30. Cree MG, Fram RY, Barr D, Chinkes D, Wolfe RR, Herndon DN. Insulin resistance, secretion and breakdown are increased 9 months following severe burn injury. Burns. 2009; 35:63–69. [PubMed: 18672331]

31. Turinsky J, Saba TM, Scovill WA, Chesnut T. Dynamics of insulin secretion and resistance after burns. J Trauma. 1977; 17:344–350. [PubMed: 870699]

32. Gustavson SM, Chu CA, Nishizawa M, Farmer B, Neal D, Yang Y, Donahue EP, Flakoll P, Cherrington AD. Interaction of glucagon and epinephrine in the control of hepatic glucose production in the conscious dog. Am J Physiol Endocrinol Metab. 2003; 284:E695–707. [PubMed: 12626324]

33. Burant CF, Treutelaar MK, Block NE, Buse MG. Structural differences between liver- and muscle-derived insulin receptors in rats. J Biol Chem. 1986; 261:14361–14364. [PubMed: 3533919]

34. Caro JF, Raju SM, Sinha MK, Goldfine ID, Dohm GL. Heterogeneity of human liver, muscle, and adipose tissue insulin receptor. Biochem Biophys Res Commun. 1988; 151:123–129. [PubMed: 3279949]

35. Gelfand RA, Barrett EJ. Effect of physiologic hyperinsulinemia on skeletal muscle protein synthesis and breakdown in man. J Clin Invest. 1987; 80:1–6. [PubMed: 3298320]

36. Nuutila P, Raitakari M, Laine H, Kirvela O, Takala T, Utriainen T, Makimattila S, Pitkanen OP, Ruotsalainen U, Iida H, Knuuti J, Yki-Jarvinen H. Role of blood flow in regulating insulin-stimulated glucose uptake in humans. Studies using bradykinin, [15O]water, and [18F]fluoro-deoxy-glucose and positron emission tomography. J Clin Invest. 1996; 97:1741–1747. [PubMed: 8601640]

37. Kelley DE, Mintun MA, Watkins SC, Simoneau JA, Jadali F, Fredrickson A, Beattie J, Theriault R. The effect of non-insulin-dependent diabetes mellitus and obesity on glucose transport and phosphorylation in skeletal muscle. J Clin Invest. 1996; 97:2705–2713. [PubMed: 8675680]

38. Selberg O, Burchert W, vd Hoff J, Meyer GJ, Hundeshagen H, Radoch E, Balks HJ, Muller MJ. Insulin resistance in liver cirrhosis. Positron-emission tomography scan analysis of skeletal muscle glucose metabolism. J Clin Invest. 1993; 91:1897–1902. [PubMed: 8486761]

39. Utriainen T, Nuutila P, Takala T, Vicini P, Ruotsalainen U, Rönnemaa T, Tolvanen T, Raitakari M, Haaparanta M, Kirvelä O, Cobelli C, Yki-Järvinen H. Intact Insulin Stimulation of Skeletal Muscle Blood Flow, Its Heterogeneity and Redistribution, but Not of Glucose Uptake in Non-insulin-dependent Diabetes Mellitus. J Clin Invest. 1997; 100(4):777–85. [PubMed: 9259575]

40. Liang C, Doherty JU, Faillace R, Maekawa K, Arnold S, Gavras H, Hood WB Jr. Insulin infusion in conscious dogs. Effects on systemic and coronary hemodynamics, regional blood flows, and plasma catecholamines. J Clin Invest. 1982; 69:1321–1336. [PubMed: 6123523]

41. James DE, Burleigh KM, Storlien LH, Bennett SP, Kraegen EW. Heterogeneity of insulin action in muscle: influence of blood flow. Am J Physiol. 1986; 251:E422–430. [PubMed: 3532818]

42. Ferguson MK, Seifert FC, Replogle RL. The effects of thermal injury on rat skeletal muscle microcirculation. J Trauma. 1982; 22:880–883. [PubMed: 7131609]

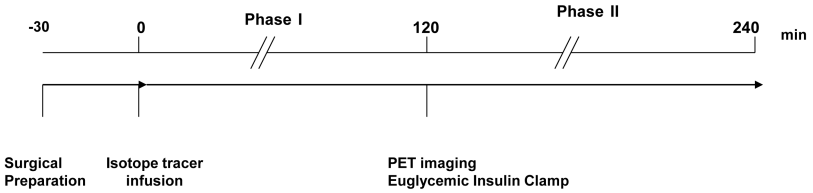


**Figure 1. Schematic representation of the experimental design**

Each experiment was preceded by surgical implantation of catheters into the left jugular vein and the left carotid artery, which took about 30 minutes. Immediately after surgery, the animal was placed in the gantry of the PET camera. Subsequently, a 2 ml baseline blood sample was taken and a primed constant infusion of stable isotope tracer was started. The stable isotopes were infused for 6 hours. Additional blood samples (2 ml each) were collected at 100, 110, 120 minute time points. Euglycemic insulin clamp was initiated at 120 minutes. Meanwhile, the PET camera was prepared for the imaging studies. Additional 2 ml blood samples were collected at 220, 230, 240 minutes.

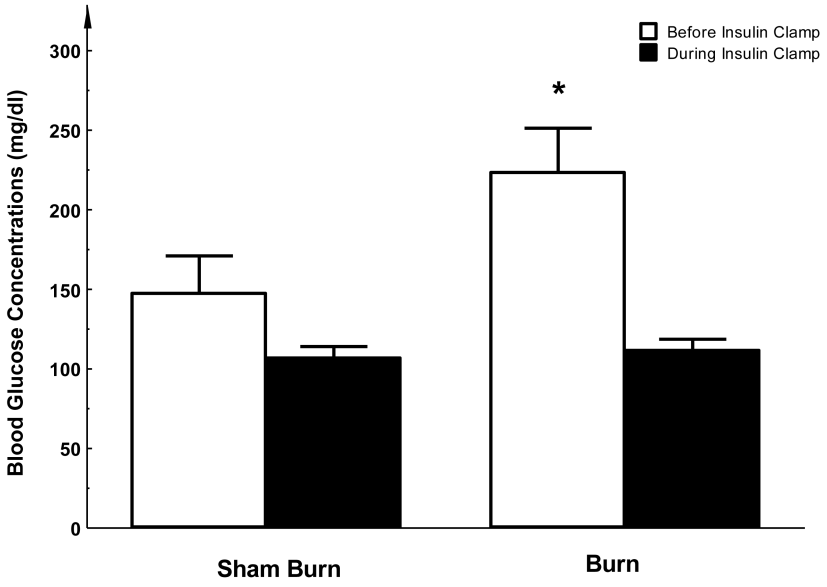


**Figure 2. Fasting blood glucose levels before and after EIC**

Before the clamp study, the level of plasma glucose was significantly higher in the burn injury group compared to sham treated animals. After insulin clamp, plasma glucose levels were maintained at a similar level in both groups. Each value is the mean ± SEM for six animals. *P < 0.05.

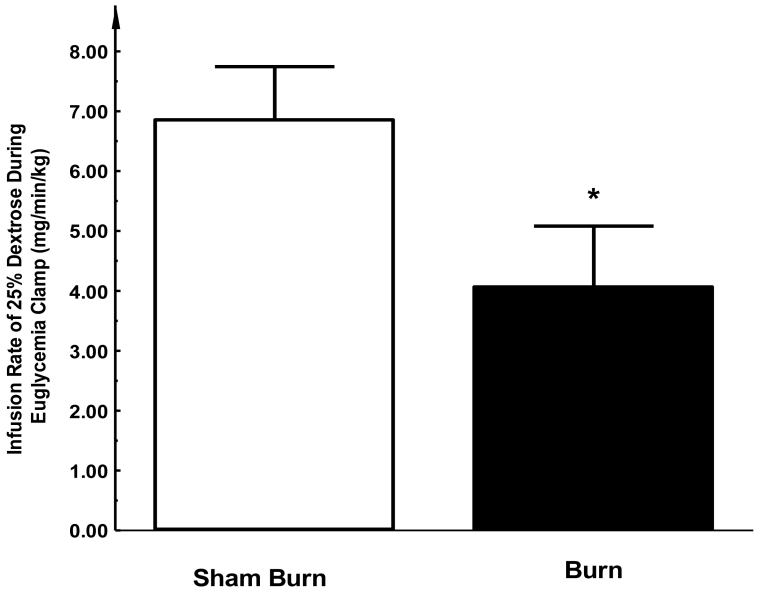


**Figure 3. Infusion rates of 25% dextrose used for maintaining euglycemia during insulin clamp study**

During insulin clamp, while insulin was continuous infused, 25% dextrose was supplied in order to maintain plasma glucose levels in the physiological range (90-110 mg/dl). In the burn group, the rates of dextrose infusion were significantly lower than that in sham group, indicating the development of an insulin resistant state. Each value is the mean ± SEM for six animals. *$P < 0.05$.

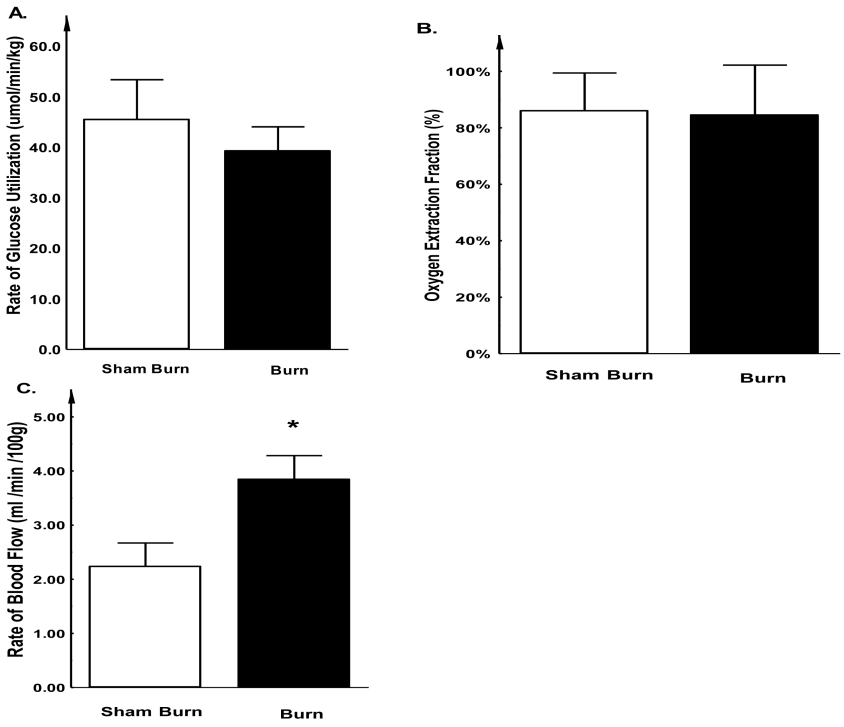


**Figure 4. Glucose uptake (A), Oxygen extraction fraction (B) and Blood flow (C) in rabbit hind-limbs**

The rabbits were positioned in the gantry of a PC-4096 PET camera with their thighs centered in the field of view. Radioactive gases were supplied via a cylindrical mixing chamber. Rabbits were studied successively with $C^{15}O_2$, $^{15}O_2$ and $^{18}$FDG. The PET study revealed that there was no statistically significant difference in glucose uptake or oxygen extraction fraction between the burn injured and sham treated control groups. However, regional blood flow was significantly increased after burn injury. Each value is the mean ± SEM for six animals. *P < 0.05.

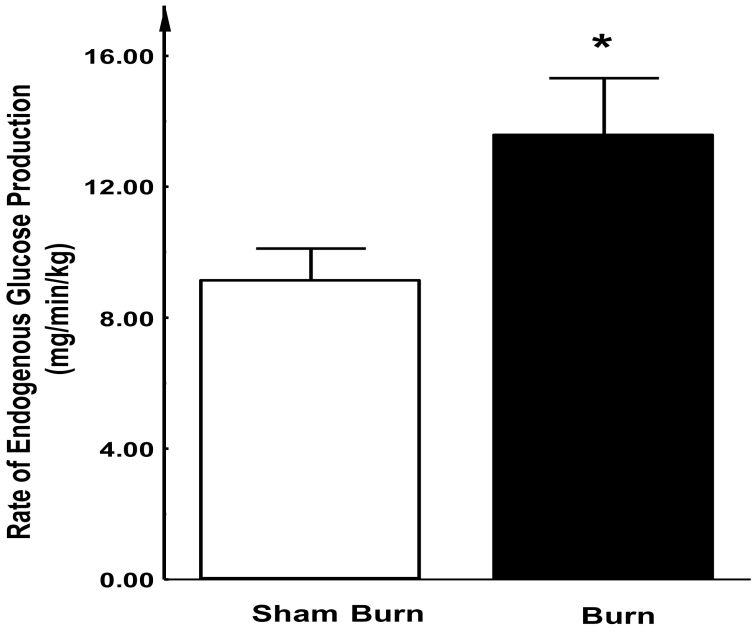


**Figure 5. Endogenous glucose production during EIC study**

During euglycemic insulin clamp study (phase II), rabbits received constant insulin infusion supplemented with various doses of 25% dextrose. Using the steady-state isotope tracer dilution approach, endogenous glucose production (i.e. gluconeogenesis) in the fasting state was determined. The levels of endogenous glucose production in burn injured rabbits remained significantly elevated compared with the sham treated control group. Each value is the mean ± SEM for six animals. *$P < 0.05$.